LARGE-SCALE ACTIVE CORONAL PHENOMENA IN YOHKOH SXT IMAGES

II. *Stationary Post-Flare Giant Arches*

FRANTIŠEK FÁRNÍK
Astronomical Institute of Czech Academy of Sciences, 25165 Ondřejov, Czech Republic
ZDENĚK ŠVESTKA
Center for Astrophysics and Space Sciences, UCSD, La Jolla, CA 92093-0111, U.S.A.
HUGH S. HUDSON
Institute for Astronomy, University of Hawaii, Honolulu, HI 96822, U.S.A.
YUTAKA UCHIDA
Physics Department, Science University of Tokyo, 1–3 Kagurazaka, Shinjuku-ku, Tokyo 162, Japan

(Received 22 March, 1996; in final form 14 June, 1996)

Abstract. We discuss *Yohkoh* SXT observations of stationary giant post-flare arches which occurred on 3–6 May, 1992 and study in detail the last arch, associated with the flare at 19:02 UT on 5 May, which extended above the west limb. The arch was similar to the first giant arch discovered on board the SMM, on 21–22 May, 1980. We demonstrate that the long lifetimes of these structures necessarily imply additional energy input from the underlying active region: otherwise, conduction would cool these arches in less than one hour and even with the unlikely assumption of conduction inhibited, pure radiative cooling would not produce the temperature decrease observed. All arch tops, although varying in brightness, stayed for several days at a fairly constant altitude of $\sim$ 100 000 km, and the arch studied, on 5–6 May, was just a new brightening of the pre-existing decaying structure. The brightening was apparently due to inflow of hot plasma from the flare region. *Yohkoh* data confirm that these stationary arches are rare phenomena when compared with the rising arches studied in Paper I and with Uchida *et al.*'s expanding active regions.

1. Introduction

In the first paper of this series (Švestka *et al.*, 1995, Paper I) we have explained the aims of the present study: an improvement of our knowledge of the phenomenon of giant post-flare arches, detected by the X-ray imaging instruments on board the Solar Maximum Mission (SMM) spacecraft, by using *Yohkoh* soft X-ray data. In Paper I we have pointed out the improvements that *Yohkoh* offers for such a research (much better spatial and temporal resolution and reduced scattered light), as well as the difficulties one encounters when trying to identify giant arches in *Yohkoh* Soft X-ray Telescope (SXT) images (too many X-ray-emitting structures associated with active regions on the disk in *Yohkoh* SXT energy range, in particular; therefore, most identifications were made on, or close to, the solar limb).

In Paper I we have identified and studied a phenomenon which was typical of most giant post-flare arches observed on the SMM either by the Hard X-ray

Solar Physics **168:** 331–343, 1996.

Imaging Spectrometer (HXIS; Švestka, 1984) or by the Flat Crystal Spectrometer (FCS; Hick *et al.*, 1987): post-flare giant arches expanding with a constant speed. However, the first giant arch discovered by HXIS on 21–22 May, 1980 (Švestka *et al.*, 1982) did not belong to this category: this arch stayed at the same altitude for at least 10 hours (Hick and Švestka, 1985). Therefore, in this Paper II we present a series of arch structures observed by *Yohkoh* on 3–6 May, 1992, in which the arches appear to be very similar to the giant arch of 21–22 May, 1980. *Yohkoh* images provide additional information about these coronal structures which SMM data could not reveal. Also, as the 21–22 May, 1980 arch was observed on the solar disk (position 13 S 15 W), the limb observations on *Yohkoh* are much more sensitive to any vertical motions in the arch and thus can verify its stationarity.

2. The Arch of 5 May, 1992

On 5 May, 1992 at 19:02 UT an SF/C6.4 flare occurred in AR 7150 at the position 8° S and 73° W, peaking in Hα at 19:12 UT and ending at 20:01 UT (*Solar-Geophysical Data*, 1992). The GOES X-ray record is complex, because several flares in different positions occurred on the Sun after 19 UT, and the long tail of decreasing X-ray flux lasting until $\sim$ 03:00 UT next day is due to another flare that appeared at 19:41 UT in AR 7154 (at 25° S and 45° E). Due to the proximity to the limb of the 19:02 UT flare the Hα flare importance was clearly underestimated, and one is unable to see whether this was a two-ribbon ('eruptive') or a compact flare.

Sagamore Hill (*Solar-Geophysical Data*, 1992) reported metric radio continuum from 21:32 UT through 22:30 UT, but its position on the disk is not known. Nevertheless, it occurred when the associated giant arch reached its maximum brightness (cf., Figure 3). A permanent noise storm was recorded on this day and on several days before by Potsdam (*Solar-Geophysical Data*), and Bogod *et al.* (1995) located its source in AR 7150 on 1 and 3 May. No measurements of the position of the noise-storm source are available on 4–8 May (cf., Section 3), but it is likely that the storm came from the same region. Also the stationary arch on 21–22 May, 1980 was accompanied by a noise storm (Švestka *et al.*, 1982).

The post-flare development in the X-ray corona can be followed in full-Sun images obtained by the SXT on *Yohkoh*. Although, due to enhanced activity close to the eastern limb, there were no partial frame images pointed at the west-limb region which we are interested in, the full-Sun images were frequent enough to provide basic information about the coronal developments following the flare.

The first post-flare X-ray image available, at 19:43 UT, shows an arch structure over the flare site, extending above the limb. The arch was then brightening until 21:36 UT and slowly decayed thereafter, completely disappearing after 14 UT on 6 May. Figure 1 shows two examples of this arch compared to X-ray contours of the HXIS stationary arch on 22 May, 1980: the HXIS images were made at 03:57 UT

and 06:51 UT (7 and 10 hours after the onset of the parent flare), the *Yohkoh* images at 00:35 UT and 05:41 UT (5.5 and 10.5 hours after the flare onset). The scale is the same in all images, and one can see the close similarity of these two coronal structures both in size and shape. The difference is that the marked scale unit of 1 arc min corresponded to two pixels of HXIS, but it corresponds to 12 pixels in *Yohkoh* images, so that the spatial resolution is 6 times better. Still, we are unable to distinguish individual loops of which the arch structure was most likely composed.

Figure 2(a) shows the altitude of the top of the arch versus time between 19:43 UT on 5 May and 10:25 UT on 6 May, 1992. The altitude has been corrected for solar rotation, under the assumption that the arch extended vertically in the east–west direction above the flare site, but was inclined by 34° to the south, as images in Figures 1 and 5 indicate. One can see a slight increase in the altitude, from about 95 000 km at 20 UT on May 4 to 113 000 km at 10 UT on May 5, but the speed of rise was decreasing from $\sim$ 1.1 km s^{-1} at the beginning of our observations to less than 200 m s^{-1} in the late phase of the arch development (Figure 2(b)). Note that the initial higher speed of rise corresponds to the period when the arch was being filled in with inflowing plasma (cf., Figure 5). For the 'stationary' arch of 21–22 May, 1980, Hick and Švestka (1985) found that the spatial resolution of 32 arc sec allowed an upper limit of 1.1 km s^{-1} for the average speed of rise of the structure, in the extreme situation when the rising top entered the pixel of maximum brightness at the very beginning and left it at the end of the 8.3 hr period of HXIS observations.

The *Yohkoh* image in Figure 1(d) shows the area A near the top of the arch, where we measured the brightness in Al.1-filter images. The results of our measurements (means of 36 pixels of 4.9 × 4.9 arc sec) are shown in Figure 3. The flux F was first measured in images with 78 ms exposure time; however, after 03:00 UT the flux in 78 ms exposures became too weak to yield statistically significant values, and we had to use 2668 ms images for our measurements. The flux decay is exponential, very approximately following the trend $\ln F = 9.40 - 0.347t$, with t in hours after 21:36 UT on 5 May.

Whenever approximately simultaneous images in Al.1 and AlMg filters (cf., Tsuneta *et al.*, 1991) were available, values of the temperature, T, and emission measure, Y, could be directly computed. The results are shown in Figure 4. Unfortunately, we could not use any ratios of 78 ms images after 23:00 UT, as the ratios became statistically insignificant, and we could not use the ratios of 2668 ms images either, as they were overexposed. Only at 03:57 UT were these images not saturated.

Figure 4 shows that the temperature T decreased from $T = 5.37 \times 10^6$ K at 21:36 UT on May 5 to $T = 2.95 \times 10^6$ K at 03:57 UT on May 6, i.e., 6^h21^m later. During the same period the volumetric emission measure Y decreased from $Y = 4.8 \times 10^{45}$ cm^{-3} to $Y = 9 \times 10^{44}$ cm^{-3}. These Y values correspond to one 4.9 × 4.9 arc sec pixel, i.e., to an area of 1.26×10^{17} cm^2. Thus, at 21:36 UT, the observed maximum linear emission measure, $Y_c = n_e^2 d$, corresponds

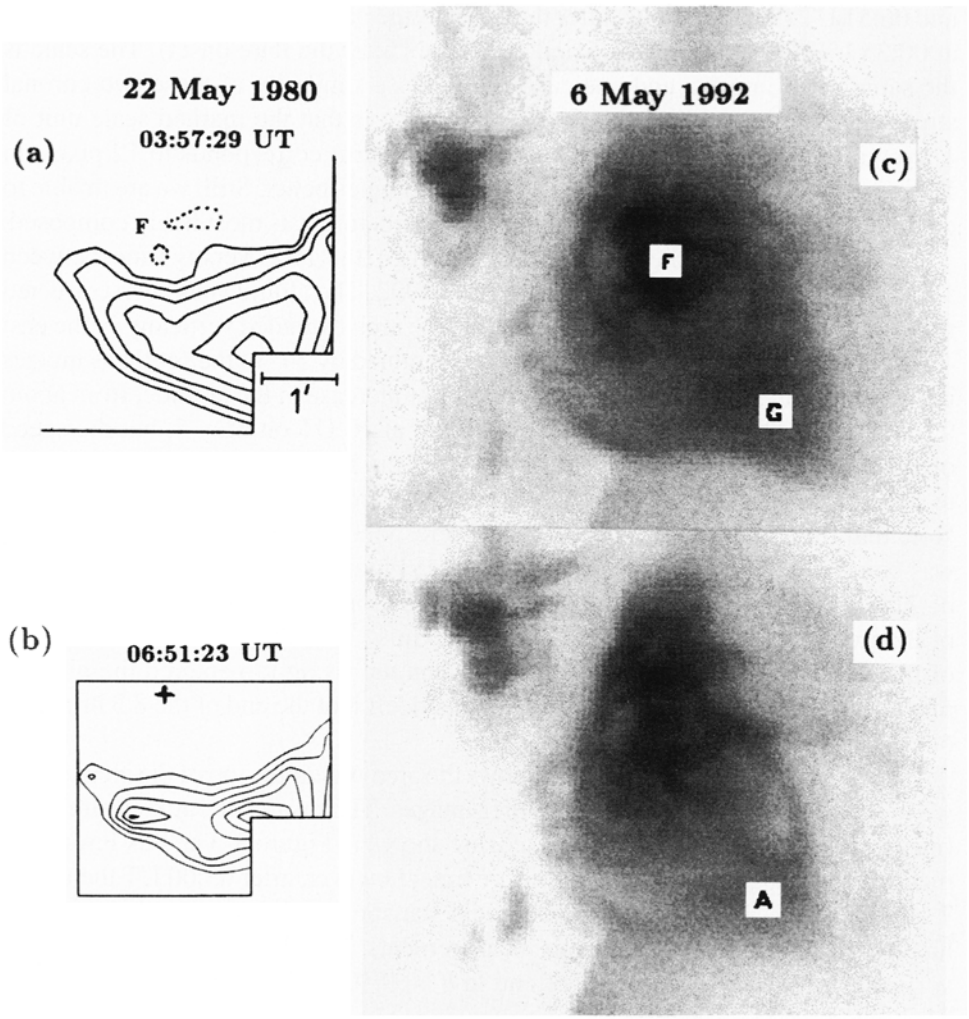

Figure 1. Left: isocontours of the stationary post-flare giant arch observed by HXIS (SMM) on 22 May, 1980 in > 3.5 keV X-rays: (a) at 03:57 UT, 7 hours after the parent flare onset (after de Jager and Švestka, 1985), and (b) at 06:51 UT, 10 hours after the flare (after Hick and Švestka, 1985). The position of the preceding flare (at 13 S 15 W) is marked by dotted contours (F) in (a) and by a cross in (b). *Right*: images of a similar arch observed by SXT (*Yohkoh*) on 6 May, 1992 in Al.1 filter in soft X-rays: (c) at 00:35 UT, 5.5 hours after the parent flare onset, and (d) at 05:41 UT, 10.5 hours after the flare. In (c), G marks the arch and F the flare site, at that time in a position 08 S 78 W. In (d), A marks the area where the flux was measured.

to 3.8×10^{23} cm^{-5}. Assuming $10^9 \leq d \leq 10^{10}$ cm, the electron density n_e is $1.9–6.2 \times 10^9$ cm^{-3}. At 03:57 UT, $6^{\mathrm{h}}21^{\mathrm{m}}$ later, $n_e = 8.0 \times 10^8–2.5 \times 10^9$ cm^{-3}.

The decrease in density may be due to a downflow of the plasma contained in the arch. Although we do not have frequent pictures in the early phase of the arch development, the observations clearly indicate that the arch brightened by

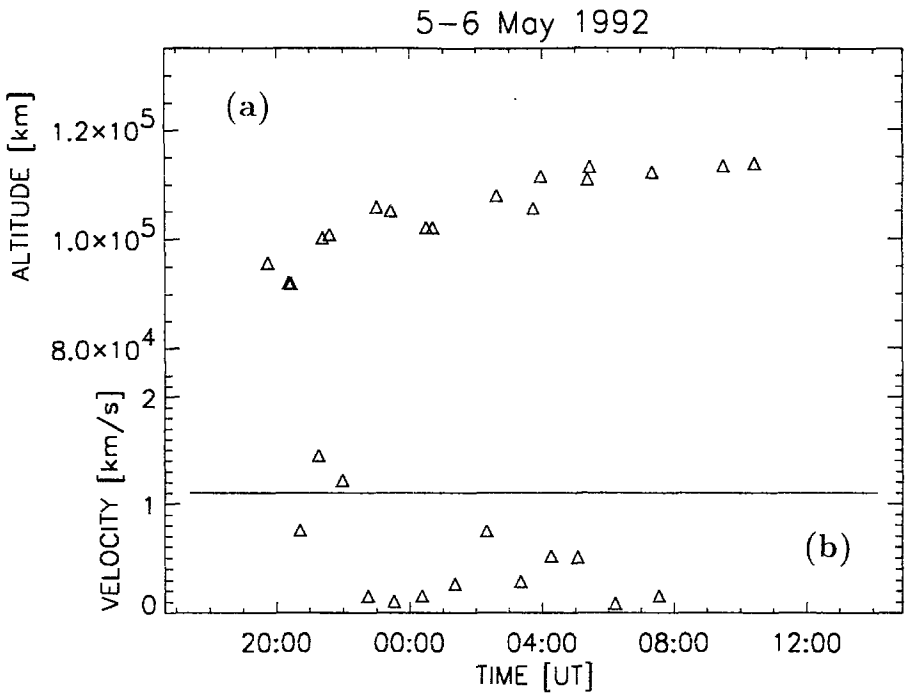

Figure 2. (a) Altitude of the brightest part of the arch of 5–6 May, 1992, corrected for solar rotation, assuming vertical extension of the arch. (b) The speed of rise of the brightest part of the arch. (Smoothed means of four subsequent data; therefore, there are no negative velocities in this graph.) The line shows the upper average-speed limit found by Hick and Švestka (1985) for the stationary arch of 21–22 May, 1980.

an inflow of hot plasma from the flare region (cf., Figure 5). This plasma may slowly return downward as the arch cools. However, the decrease in emission measure does not necessarily imply decreasing electron density. The arch most probably consists of many loop-like substructures, which may cool differently (due to different n_e values, or because of deviations from classic conduction in some of them). Thus, after more than 6 hours of cooling, large portions of the arch might not be recognizable in the Al.1 filter any longer, and the d value at 04:00 UT thus becomes much smaller than at the time of the observed maximum. Therefore, let us first consider the case when n_e is constant in time.

We will adopt the lowest $n_{e\max}$ value obtained for the maximum emission measure, 1.9×10^9 cm^{-3}. This corresponds to $d = 100\,000$ km at the time of the observed maximum Y value and 19 800 km at 03:57 UT. For constant n_e and temperature within $3 \times 10^5 < T < 3 \times 10^7$ K one can use the simplified formula for combined conductive and radiative cooling (Švestka, 1987)

$$t_c = \int_{T_{\max}}^{T(t_c)} T^{1/2}\, \mathrm{d}T/(a + bT^4)\,, \tag{1}$$

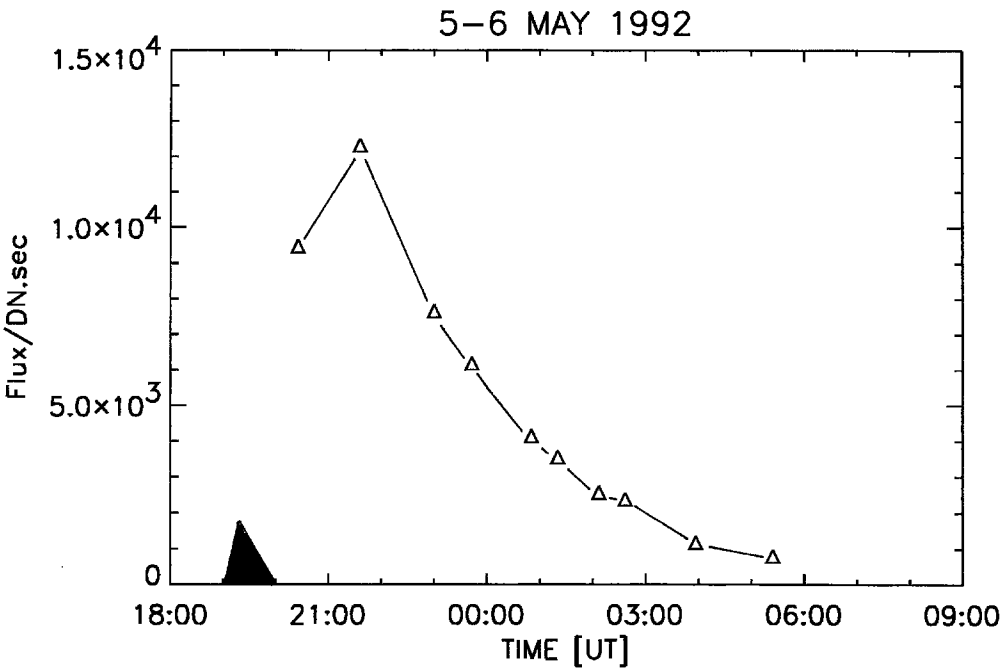

Figure 3. Flux near the top of the arch (in the area A in Figures 1(d) and 5) through the Al.1 filter. The real flux maximum probably occurred between the two values measured at 20:25 UT and 21:36 UT. The black triangle indicates the onset, maximum, and end of the parent flare.

with $T(t_c) = 2.95 \times 10^6$ K and $T_{\max} = 5.37 \times 10^6$ K, where

$$a = 2.9 \times 10^{-4} n_e \tag{2}$$

characterizes the radiative losses, and

$$b = 2.66 \times 10^9 / n_e L^2 \tag{3}$$

the conductive cooling. t_c is the cooling time from the maximum temperature $T_{\max}$ to a temperature at time t_c, $2L$ is the length of the loop (approximated as πh, where h is the altitude of the top of the arch), and the temperature gradient within the loop, ∇T, is taken as $\nabla T = T/L$.

Providing that there has been no additional energy input into the arch structure, it is easy to demonstrate that the cooling process in the arch is too slow to allow for full classical conductive cooling. Differentiating Equation (1), one finds that the maximum duration of cooling from 5.37×10^6 K to 2.95×10^6 K occurs in the interval 1.5×10^9 cm$^{-3} < n_e < 5.1 \times 10^9$ cm^{-3}. Exact computations find the maximum cooling time $t_{c\max} = 46.0$ min at $n_e = 2.7 \times 10^9$ cm^{-3}. For any higher or lower n_e value the cooling time is shorter. Thus, for combined radiative and conductive cooling, one can never get the observed value of $t_c = 6.35$ hours.

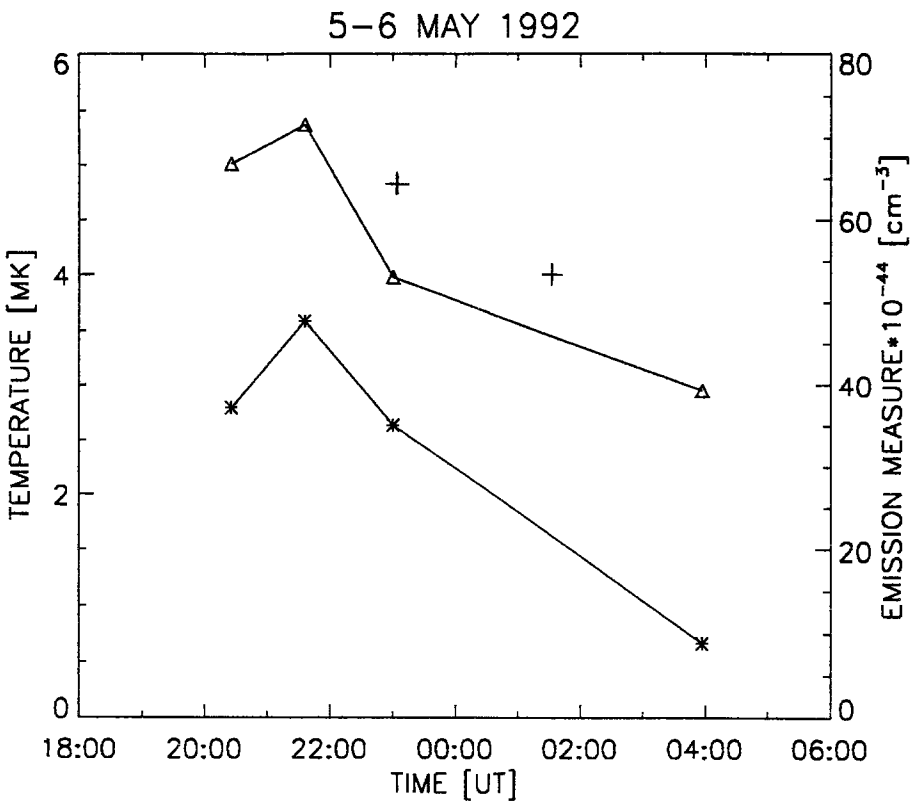

Figure 4. *Triangles*: temperature variations near the top of the arch (area A in Figure 1(d)) deduced from the flux ratios in Al.1 and AlMg filters (cf., Tsuneta *et al.*, 1991). *Asterisks*: emission measure variations in the same area, per one pixel of 4.9 × 4.9 arc sec, deduced from the same Al.1/AlMg ratios and the Al.1 flux measured. *Crosses*: temperature values corresponding to pure radiative cooling from $T = 5.37 \times 10^6$ K at 21:36 UT on May 5 to $T = 2.95 \times 10^6$ K at 03:57 UT on May 6.

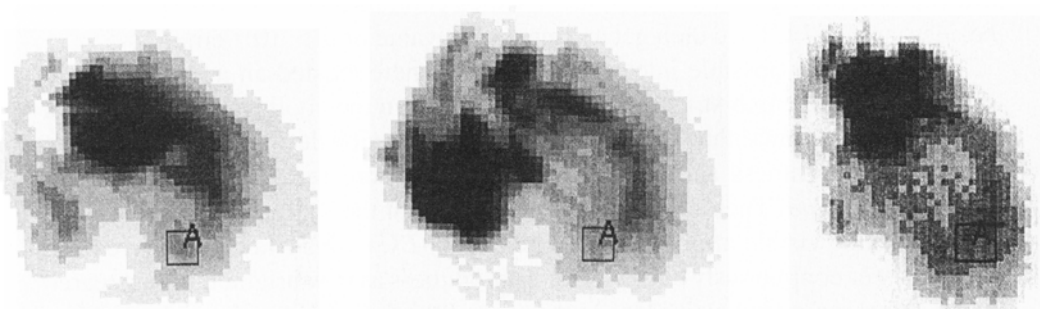

Figure 5. Brightening of the arch through inflow of hot plasma from below. *From the left*: 20:25:17 UT; 21:35:57 UT; 23:25:51 UT. (78 ms exposures, filter Al.1.) Note that the inflow period corresponds to the higher 'speed of rise' in Figure 2.

In order to get such a t_c value, one has to diminish the value of b in (3), i.e., to slow down the classical conduction process. It was already argued for the giant arches observed on board the SMM that conduction should not play any significant role in the process of the giant-arch cooling, because otherwise the arch would cool so fast that a continuous supply of energy would be needed to keep the arch visible in X-rays for so many hours (Švestka, 1984; also see Paper I). Therefore, let us assume the extreme case that the conduction is fully inhibited and that the arch cools only through radiative losses. Then Equation (1) simplifies to

$$t_c = 2.30 \times 10^3 n_e^{-1} T_{\max}^{3/2} [1 - (T_c/T_{\max})^{3/2}] , \tag{4}$$

and for $t_c = 6.35$ hr the electron density is found to be $n_e = 7.4 \times 10^8$ cm $^{-3}$. For the same n_e value, Equation (1), including conduction, yields $t_c = 25.2$ min. However, the temperature decrease obtained from (4) for pure radiative cooling at constant n_e, shown as crosses in Figure 4, does not correspond to the temperature decrease observed. As Figure 4 demonstrates, in the early phase of the cooling process the temperature decrease was much faster than Equation (4) prescribes for constant $n_e = 7.4 \times 10^8$ cm^{-3}.

In order to explain this discrepancy one could suggest that either the electron density n_e was decreasing during the cooling process, or some conduction was involved during the initial phase of the cooling in some components of the arch structure. Both these explanations imply that some loop components of the arch cooled faster than those which stayed visible 6.35 hours later. Indeed, the T decrease from 21:36 UT to 23:00 UT requires $n_e \leq 1.47 \times 10^9$ cm^{-3} (where the equality refers to pure radiative cooling), whereas that from 23:00 UT to 03:57 UT needs $n_e \leq 2.44 \times 10^8$ cm $^{-3}$. With this very low density in the later phase of development, however, the corresponding Y values lead to an increase of the geometrical thickness, d, during the cooling process, which contradicts the above expectations; besides, at 03:57 UT we then get an impossible value of $d > 10^{11}$ cm.

Thus the only possible interpretation is that there existed an additional input of energy into the arch structure which slowed down the cooling process. Indeed, *Yohkoh* images show enhanced activity in the active region during the whole decline of the arch brightness and several tiny subflares were reported there in *Solar-Geophysical Data*. Therefore, one can conclude that the stationary arch structure, which became visible after the C6.4 flare of 19:02 UT on 5 May, must have been repeatedly or continuously enhanced in its brightness as new brightenings appeared in the active region below it. Also in the case of the stationary arch of 21–22 May, 1980, observed by HXIS, we detected several additional brightenings in the active region underlying the arch during the arch decay (cf., Švestka *et al.*, 1982). Thus that arch, like the presently studied one, could have been fed by additional inputs of energy.

3. Structures Preceding the Event of 5 May

A structure similar to the arch discussed in the preceding section was recognizable above AR 7150 also before 19:02 UT when the flare of 5 May, 1992 began. One can see it from about 05 UT on 5 May and it apparently originated in association with one of the subflares reported in *Solar-Geophysical Data* (1992) in the morning hours of 5 May (most likely the SN flare at 04:37 UT). Although this structure varied in brightness, it was slowly decaying until the onset of the 19:02 UT event. Somewhat surprisingly, it did not react in any striking way to the appearance of the 1F/C2.0 flare that appeared in AR 7150 at 15:10 UT. It seems that the location of an energy release in the active region is more important for the energy input into the arch than the amount of energy involved (i.e., the flare importance) if the energy imput is episodic.

Prior to that, before 15 UT on 4 May, another arch-like structure could be seen above AR 7150. While the arch, discussed in the preceding section, extended toward SW, the earlier arch extended toward NW, but both arches had about the same altitude (Table I). The first arch was also stationary in nature, and it is likely that it originated during the flare that began at 08:51 UT on 3 May (*Solar-Geophysical Data*, 1992): this was a two-ribbon (eruptive) flare of importance 1 in Hα and M1.0 in X-rays, accompanied by a loop prominence system and Type II radio burst. It was the first major flare in AR 7150. Repeated activity in AR 7150 later on 3 and 4 May had to contribute to the energy input into the arch to keep it visible for 30 hours, in a similar way as we concluded for the arch studied in the preceding section. Several smaller flares and subflares during that period demonstrate continuing activity in the active region.

Unfortunately, it is essentially impossible to study in any detail the development of these arch structures prior to late hours on 5 May, because their extension was projected onto the X-ray emission of AR 7143 located about 20° to the west of AR 7150; both active regions were at the same latitude (5°–7° S for AR 7143 and 5°–8° for AR 7150.) Essentially all full-disk *Yohkoh* images during this period had low 'quarter' resolution of $\sim$ 10 arc sec which makes the separation between the arch and the active region behind it still more difficult. Only after AR 7143 disappeared behind the limb, shortly after noon UT on 5 May, did observations of the arch structure became reliable. Nevertheless, on very few exceptional occasions when the arch top brightened one can estimate the altitude of the arch structures (assuming vertical extension in the east–west direction and taking into account the observed inclination toward south or north as well as solar rotation) and the results are shown in Table I.

The fact that these two permanent arch structures stayed for tens of hours at about the same altitude close to 100 000 km is good evidence that the stationary arches are different from systems of post-flare loops that rise slowly into the corona. In the stationary arch of 21–22 May, 1980 observed by HXIS on the SMM, this fact was quite clear, because one could see at the same time both the loops below

Table I
Altitudes of the top of the arch structures on 4–6 May, 1992

Day	Time	Altitude	Remark
4 May	04:39 UT	92 000 km	First arch, toward NW
5 May	14:50 UT	92 900 km	Second arch, toward SW
5 May	16:20 UT	95 200 km	Second arch, toward SW
5 May	18:53 UT	100 000 km	Second arch, toward SW
5 May	21:30 UT	100 000 km	Brightened arch (Section 2)
6 May	10:00 UT	113 000 km	Brightened arch (Section 2)

and the arch above them (Švestka *et al.*, 1982). Here, this additional evidence is helpful, as we did not see the loops.

As we already mentioned in Section 2, during the time when these two arches existed, Potsdam reported a permanent Type I radio noise storm on the Sun. Bogod *et al.* (1995), using the VLA, localized its source above AR 7150, studied in this paper, on May 1 and 3. Unfortunately, no measurements of its position are available during the period of our study until May 9, when AR 7150 already disappeared behind the western limb and when radio noise storm came from another active region, much more to the east. Nevertheless, Bogod *et al.*'s observations indicate that the source of the Type I noise storm was in the structures observed above AR 7150 and discussed in this paper. The stationary arch of 21–22 May, 1980 was also accompanied by a radio noise storm (Švestka *et al.*, 1982) and Type I noise storms were also found in some other cases to coincide with high-lying soft X-ray structures (e.g., Lantos *et al.*, 1981). Klein *et al.* (1983) reported associations of moving Type IV bursts with hard X-rays, and stationary Type IVs (which may develop into noise storms) with soft X-rays. Similar observations also come from *Yohkoh* (on 30 July, 1992 by Krucker *et al.*, 1995 and on 6–9 May, 1993 by Bogod *et al.*, 1995).

One of the basic problems that we encountered in HXIS images was the origin of the stationary arch: how did the arch appear at such a high altitude less than 1.5 hour after the flare, staying at an almost constant altitude thereafter? Hick and Švestka (1985) found that the arch of 21 May, 1980 would have to rise with an average speed of > 17 km s^{-1} if starting at an altitude of 50 000 km, and in our case, when the arch was seen at 95 000 km altitude 40 min after the flare onset, the average speed of rise would be > 19 km s^{-1} with the same starting altitude. The speeds would be still higher if the rise started lower in the corona.

The *Yohkoh* data reveal that the arch, seen after 19:02 UT on 5 May, 1942, was already present before, and the observed brightening of this pre-existing structure was caused by inflow of hot material from below into the arch structure as demonstrated in Figure 5. Plasma flow from the chromosphere to the top of the loop should propagate with average speed of > 40 km s^{-1}. The same explanation might

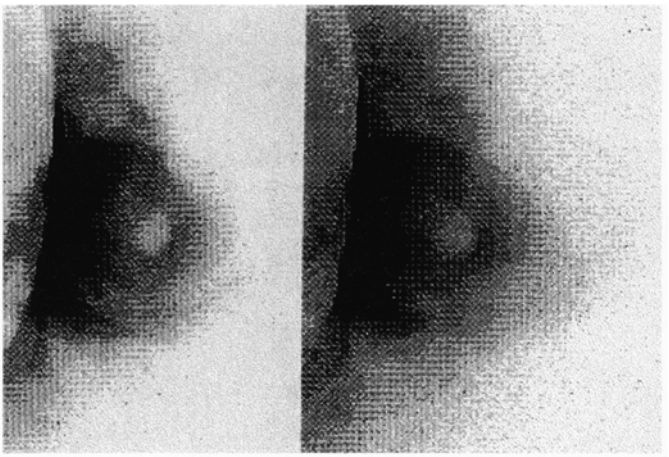

Figure 6. The giant loop structure observed above AR 7150 on 8 May after it crossed the west limb. *Left*: 01:35:08 UT. *Right*: 02:04:06 UT. (2688 ms exposures, filter A.1.)

be true for the HXIS arch of 21–22 March, 1980, because there, at much higher energies, we might not have imaged, and thus could not recognize, the pre-existing structure. However, this does not answer the question how ultimately the arch had been formed and, unfortunately, earlier *Yohkoh* images, projected on another active region, do not allow us to solve this problem either.

4. Structures Following the Event of 5 May

The arch structure, though apparently fed with additional energy input(s) during its decay on 6 May, essentially disappeared after 14 UT on 6 May and following images of the active region, crossing the west limb, did not change until 22 UT on 7 May. The region stayed bright, but no more arches were seen above it. However, between 22:10 UT and 23:45 UT on 7 May a big loop began to appear above the limb (Figure 6).

This was a completely different coronal structure, much higher than the stationary arches described in the previous sections. The loop 'eye' was at an altitude of $\sim$ 145 000 km and did not significantly change its altitude. At 02:04 UT on 8 May the top of the loop structure extended up to $\sim$ 350 000 km. The loop top further expanded upward, the structure got progressively weaker, and disappeared between 02:56 HT and 04:45 UT on 8 May; at 04:45 UT only the 'loop legs' remained visible.

This high and relatively short-lived structure differs from both the stationary and rising giant arches described in the present paper and in Paper I. It is an example of completely different large-scale coronal structures associated with active processes on the Sun, some of which we will discuss in Papers III and IV of this series.

5. Conclusions

Stationary giant post-flare arches occurred on 3–6 May, 1992 on the western solar hemisphere. We could study in more detail only the last arch, associated with the flare at 19:02 UT on 5 May, which extended above the west limb. This arch (Figure 1) was similar to the first giant arch discovered by HXIS on board the SMM, on 21–22 May, 1980 (Švestka *et al.*, 1982).

All arch tops, while varying in brightness, stayed for several days at a fairly constant altitude of $\sim$ 100 000 km (Table I), and the arch studied, on 5–6 May, was just a new brightening at the location of a pre-existing decaying structure. The brightening was apparently due to inflow of hot plasma from the active region (Figure 5). Although the top of this last arch very slowly rose in its initial phase (possibly reflecting the plasma inflow), later on the rise speed did not exceed 200 m s^{-1} (Figure 2).

The long lifetimes of these stationary structures (Figure 3) necessarily imply additional energy input from the underlying active region: otherwise, conduction would cool these arches in less than one hour and, even if for some reason conduction were inhibited, pure radiative cooling would not produce the temperature decrease that has been observed (Figure 4).

While we easily found 6 events of rising post-flare giant arches in *Yohkoh* SXT data (cf., Paper I) and surely more could have been discovered if there were no long gaps in full-disk *Yohkoh* data after major flares, we were so far able to find only one other *Yohkoh* event which may be interpreted as a series of stationary arches, on 19–21 November, 1991. Thus, obviously, these stationary arches are much rarer phenomena then the rising arches studied in Paper I. This agrees well with findings on the SMM: out of 10 giant arches discovered either by HXIS or FCS only one arch was stationary (the first one ever detected, on 21–22 May, 1980), whereas at least 6 (and possibly all remaining 9) were rising arches (cf., Hick, 1988). Obviously, expanding processes in active regions, both following flares (Paper I) and possibly independent of flaring (Uchida *et al.*, 1992), are more common on the Sun than the stationary structures discussed in this paper.

The question arises whether the stationary arches are the same phenomena as rising arches, just with speeds of rise unusually slow (as has been supposed when evaluating SMM data), or whether we encounter different physics here. In Paper I we interpreted the rising arches as expanding active-region loops left over behind coronal mass ejections. These could therefore be identifiable with the 'post-CME loops' discussed in the interplanetary community (e.g., Kahler, 1992). This interpretation can hardly be applied to stationary arches. Also, in *Yohkoh* data the temperature found in the stationary arch significantly exceeds that in the rising arches (compare present Figure 4 and Table III in Paper I). Thus it can be that the two phenomena really are different in their nature.

Acknowledgements

Thanks are due to the *Yohkoh* SXT Team for making this study possible, to Drs David Alexander, Nariaki Nitta, and Sam Freeland for their friendly help to FF and ZŠ during the data collection and evaluation, and to Prof. Y. Ogawara and his staff for kind support during visits of FF and ZŠ at ISAS. Very useful comments by an unknown referee helped to improve the presentation. The work of FF was supported by Grant No. 303404 of the Grant Agency of the Academy of Sciences of the Czech Republic and the work of ZŠ by Contract No. ATM-9312023 with the US National Science Foundation.

References

Bogod, V. M., Garimov, V., Gelfreikh, G. B., Lang, K. R., Willson, R. F., and Kile, J. N.: 1995, *Solar Phys.* **160**, 133.
De Jager, C. and Švestka, Z.: 1985, *Solar Phys.* **100**, 435.
Hick, P.: 1988, 'Interpretation of Energetic Phenomena in the Solar Corona', Thesis, University of Utrecht.
Hick, P. and Švestka, Z.: 1985, *Solar Phys.* **102**, 147.
Hick, P., Švestka, Z., Smith, K. L., and Strong, K. T.: 1987, *Solar Phys.* **114**, 329.
Kahler, S.: 1992, *Ann. Rev. Astron. Astrophys.* **30**, 113.
Klein, L., Anderson, K., Pick, M., Trottet, G., Vilmer, N., and Kane, S.: 1983, *Solar Phys.* **84**, 295.
Krucker, S., Benz, A. O., Aschwanden, M. J., and Bastian, T. S.: 1995, *Solar Phys.* **160**, 151.
Lantos, P., Kerdraon, A., Rapley, G. G., and Bentley, R. D.: 1981, *Astron. Astrophys.* **101**, 33.
Solar-Geophysical Data: 1992, No. 574, Part I, No. 575, Part I, No. 579, Part II.
Švestka, Z.: 1984, *Solar Phys.* **94**, 171.
Švestka, Z.: 1987, *Solar Phys.* **108**, 411.
Švestka, Z., Stewart, R. T., Hoyng, P., van Tend, W., Acton, L. W., Gabriel, A. H., and 8 co-authors: 1982, *Solar Phys.* **75**, 305.
Švestka, Z., Fárník, F., Hudson, H. S., Uchida., Y., Hick, P., and Lemen, J. R.: 1995, *Solar Phys.* **161**, 331 (Paper I).
Tsuneta, S., Acton, L., Bruner, M., Lemen, J., Brown, W., Caravalho, R., Catura, R., Freeland, S., Jurcevich, B., Morrison, M., Ogawara, Y., Hirayama, T., and Owens, J.: 1991, *Solar Phys.* **136**, 37.
Uchida, Y., McAllister, A., Strong, K. T., Ogawara, Y., Shimizu, T., Matsumoto, R., and Hudson, H. S.: 1992, *Publ. Astron. Soc. Japan* **44**, L155.